Supporting Information

Molero et al. 10.1073/pnas.0912171106

SI Materials and Methods

Tissue Processing and Immunostaining. Tissue samples for immunohistochemistry were fixed in 4% paraformaldehyde (PFA), sucrose cryoprotected, flash frozen and cryosectioned at 12 μm. Incubation with primary antibodies were performed at specific dilutions: BrdU (Novo-Castra Laboratories) 1:200; β-tubulin (Sigma) 1:700, Calbindin (CB) (Sigma) 1:200; DARPP32 (Santa Cruz Biotechnology) 1:50; GFAP (Sigma) 1:700; Islet1 (Iowa Developmental Hybridoma Bank), 1:100; Ki67 (Novo-Castra Laboratories) 1:100; Mash1 (BD PharMingen) 1:100; mGluR1 (Chemicon) 1:100; Nanog (R&D Systems) 1:50; Nestin (BD PharMingen) 1:100; NeuN (Chemicon) 1:100; μ-Opioid Receptor-1 (Immunostar Inc) 1:500; O4 (Sigma) 1:700; RC2 (Iowa Developmental Hybridoma Bank) 1:10, Sox2 (R&D Systems) 1:500; Oct4 (Cell Signaling) 1:100. Alexa-fluor-conjugated secondary antibodies (Invitrogen) were diluted at 1:1500. Tissue sections were visualized with an Olympus BX51 microscope and photographed with a Sensicam digital camera (Cooke Corporation). E15.5 brains used for electron microscopy were fixed for 1 h in a solution composed of 2% PFA per 2.5% glutaraldehyde in 0.1M cacodylate buffer and then rinsed in buffer. Next, samples were osmicated for 1 h, and then incubated with 2% uranyl acetate for 1 h, dehydrated, and embedded in Epon LX112. Telencephalon samples at coronal level #5 [from Schambra's atlas (1992)] were then thin-sectioned and post-stained with 0.5% uranyl acetate per 0.5% lead citrate. Micrographs were taken at magnification, ×5,000.

Neural Cell Clonal Assays. Primary and secondary neural cell clones were cultured in suspension for 7 DIV in complete medium supplemented with bFGF (10 ng/mL). Secondary clones were generated by further dissociation of primary clones, followed by a second round of clonal expansion. Thereafter, 10 fields were randomly chosen and photographed. The number of clones per field and their size (area occupied by individual clones) were determined with the assistance of MicroSuite Five Biological Suite (Olympus). Each data point represents the mean of at least four independent biological experiments. The clonal differentiation assay was performed by plating primary neural clones on 1 cm^2 polyD-lysine coated glass coverslips at a density of 30 clones/plate in neurobasal medium (Invitrogen) supplemented with B27 (BD Biosciences), 5 μg/mL laminin and 50 ng/mL of BDNF (Biovision). After 7 DIV, clones were immunostained for the neural lineage markers, β-tubulin (for neurons), O4 (for oligodendrocytes), and GFAP (for astrocytes).

Subcellular Fractionation and Protein Immunoblot Analysis. Individual antibody dilutions were: Laminin B1 (Abcam), 1:2,000; Nanog (Millipore) 1:500; Oct4 (Cell Signaling) 1:500; Smad1 (Abcam) 1:1,000; Sox2 (Abcam) 1:500 and Stat3 (Cell Signaling Technology) 1:1,000.

Quantitative Real-Time PCR Analysis. Primers and probes were purchased from PE Applied Biosystems. The data collection and their quality assessment were performed using 7000 SDS 1.1 RQ Software (Applied Biosystems) and the analysis with the Relative Expression Software Tool (REST) V2.0.7 developed by Corbett Research (1).

1. Pfaffl MW, Horgan GW, Dempfle L (2002) Relative expression software tool (REST) for group-wise comparison and statistical analysis of relative expression results in real-time PCR. *Nucleic Acids Res* 30:e36.

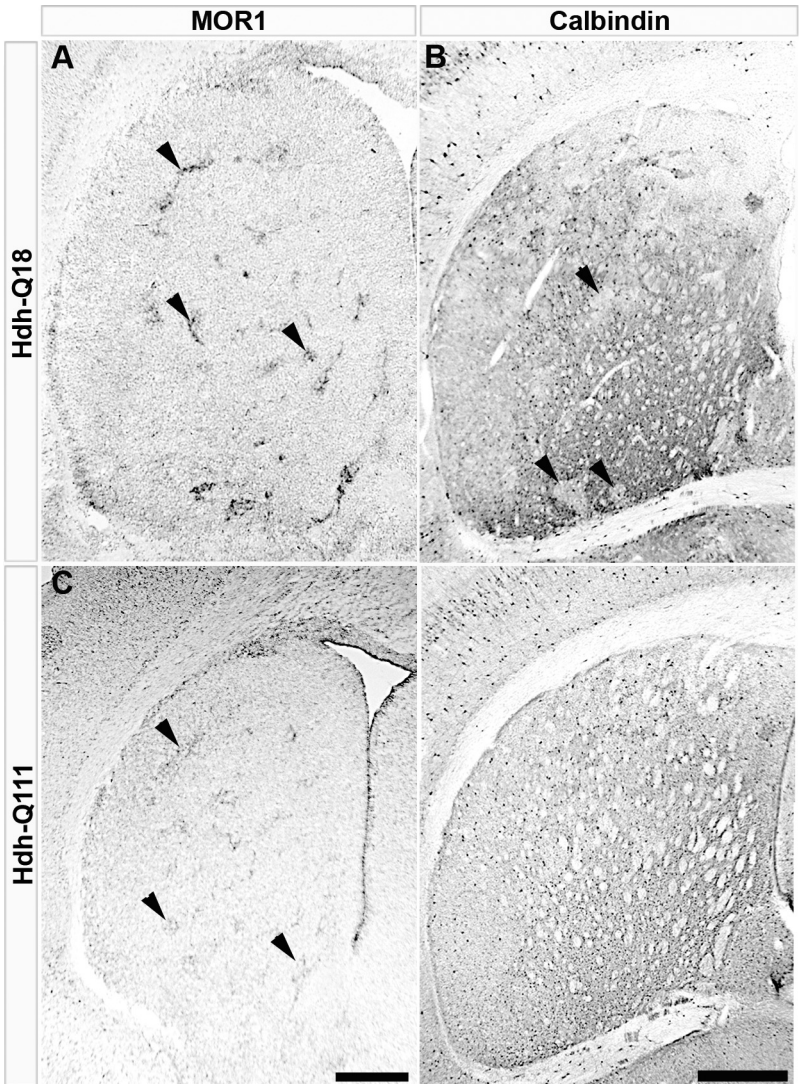

Fig. S1. Chemoarchitectural profiles of the early postnatal Hdh-Q111 striatum indicate a maturational delay. PND2 Hdh-Q111 striatum displayed the expected patchy MOR1 expression profile (*A* and *C*), although the immunoreactivity of this marker was visibly reduced in Hdh-Q111 embryos (arrowheads). PND7 Hdh-Q111 striatum lacked the CB mosaic expression profile (*B* and *D*, arrowheads). (Scale bar,200 μm in *C* and 500 μm in *D*.)

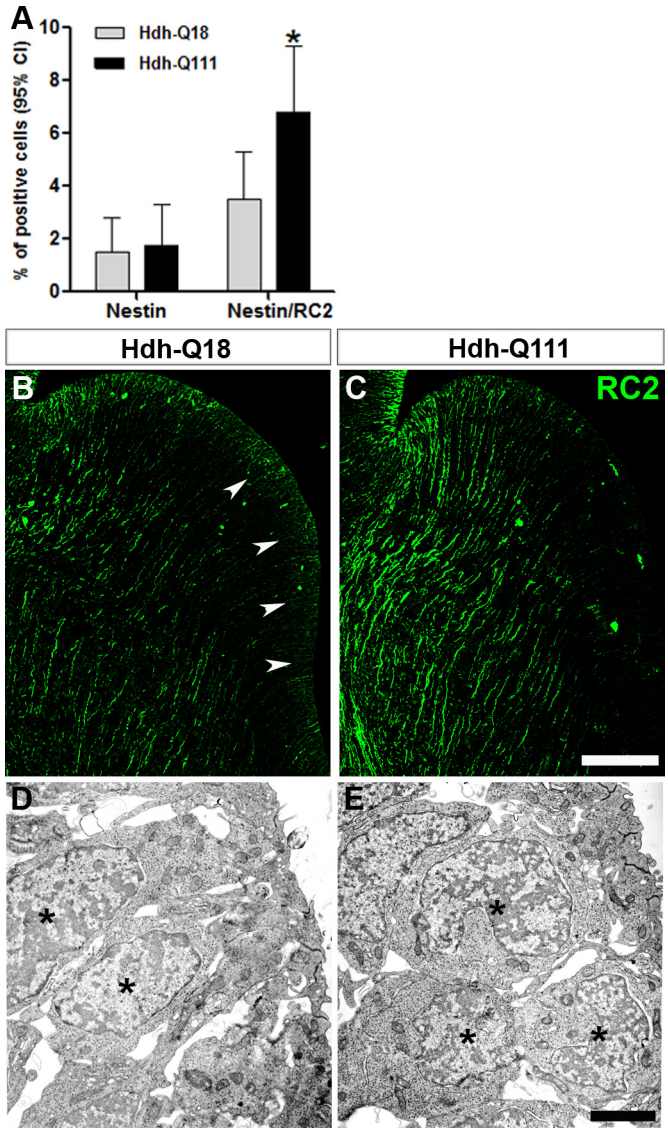

Fig. S2. Radial glial intermediate progenitors are increased in the E15.5 Hdh-Q111 striatal anlagen but are notably reduced in the medial aspect of the VZ. Quantification was performed by E15.5 striatum primordia tissue dissociation followed by culture incubation for 30 min and subsequent immunostaining for Nestin and RC2 (*A*). Bars represent the percentage ± 95% CI of immunoreactive cells; *, *P* value corresponds to <0.05. Comparative immunohistochemical analysis of Hdh-Q18 (*B*) and Hdh-Q111 (*C*) specimens revealed an overall increase of the radial glia marker, RC2 in the Hdh-Q111 mantle in association with a reduction for this marker in the VZ (arrowheads denote the Hdh-Q18 VZ). Ultrastructural microscopy of putative radial glial cells within the VZ of Hdh-Q18 specimens (*D*, asterisk), whose numbers are reduced and replaced by rounded cells with abnormal nuclear architectures in Hdh-Q111 specimens (*E*, asterisk). (Scale bar, 200 μm in *C* and 2 μm in *E*.)

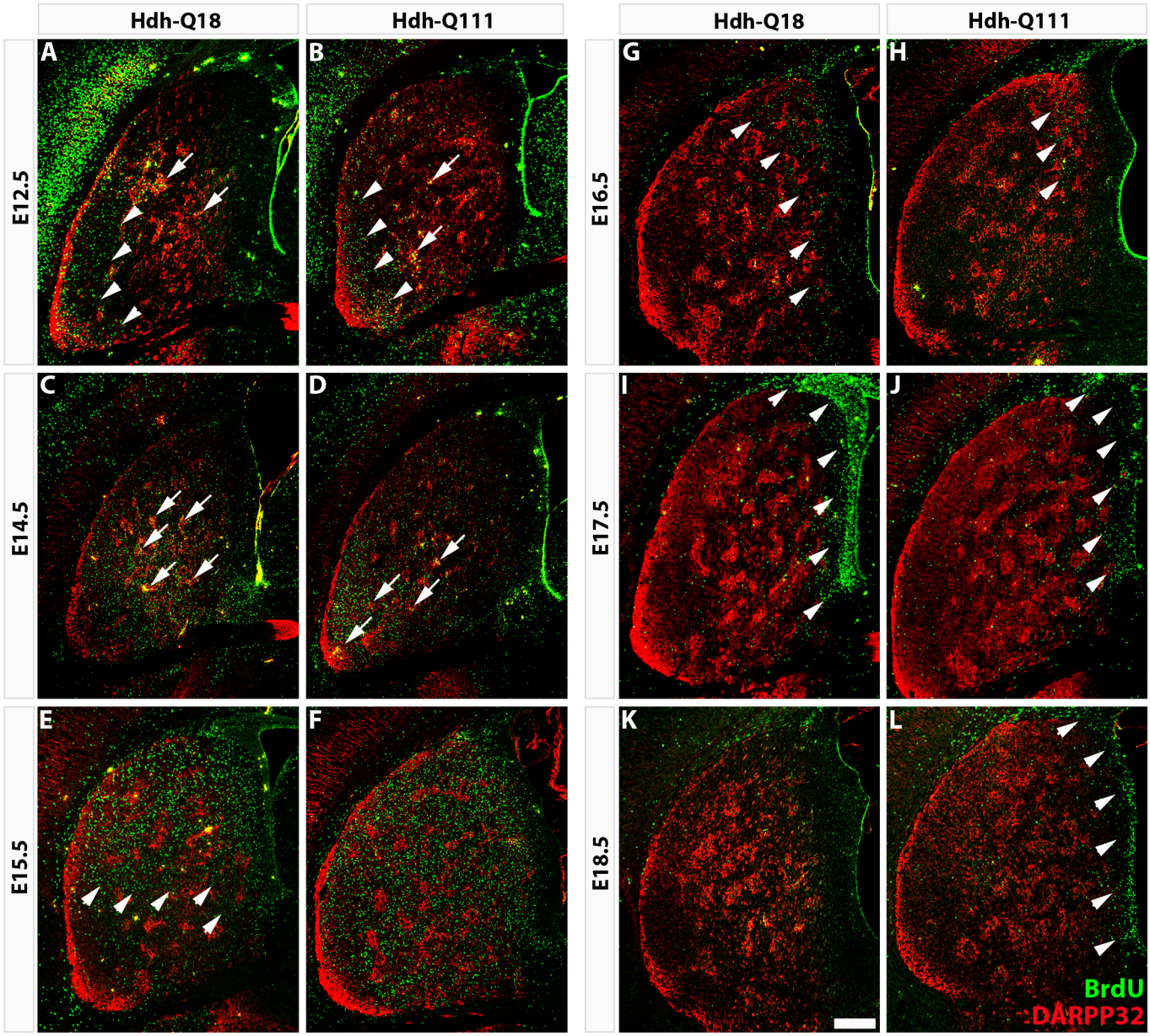

Fig. S3. Impaired spatiotemporal profiles of striatal neurogenesis in Hdh-Q111 embryos. Birth-dating analysis was performed by applying a BrdU pulse at E12.5 (*A* and *B*), E14.5 (*C* and *D*), E15.5 (*E* and *F*), E16.5 (*G* and *H*), E17.5 (*I* and *J*), and E18.5 (*K* and *L*), and brains were subsequently harvested at PND2. Arrows (*A*–*D*) point to BrdU+ cells localized in the DARPP32 immunoreactive patch compartment. Arrowheads (*A*–*L*) point to the ventrolateral to dorsomedial spatiotemporal gradient of striatal cell elaboration. (Scale bar, 200 μm in *K*.)

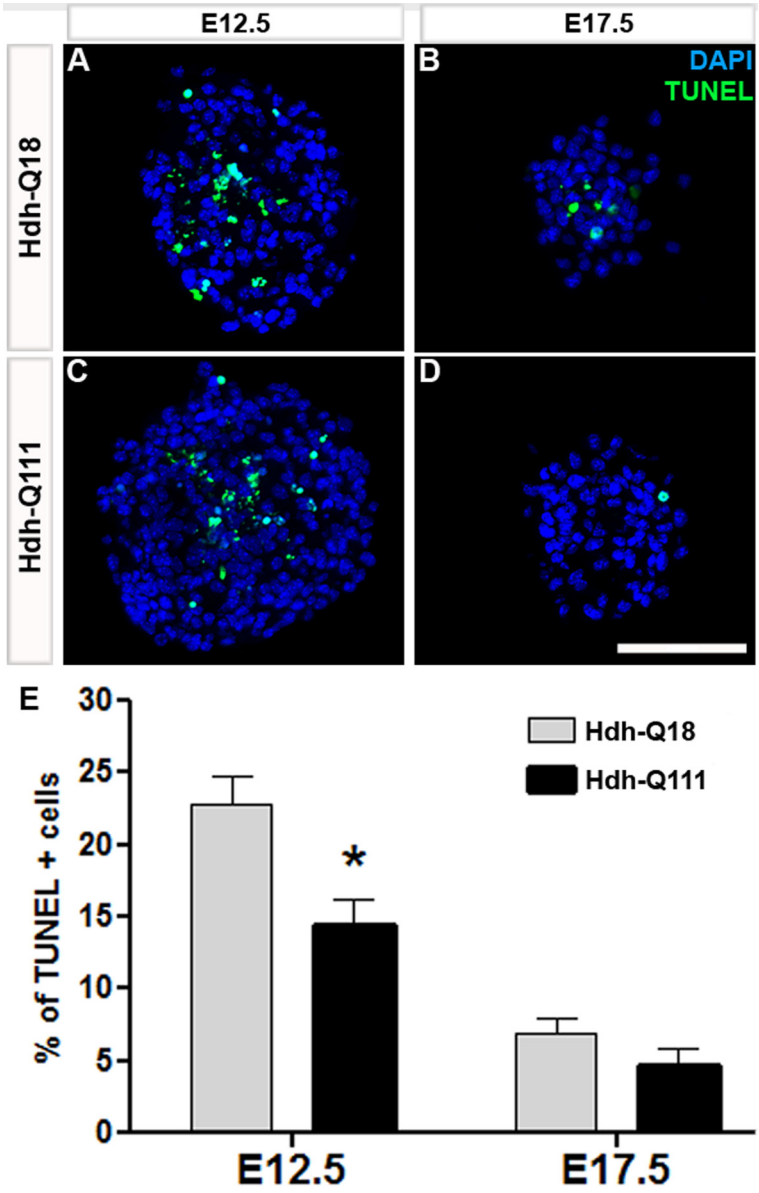

Fig. S4. Presence of apoptotic cells in primary Hdh-Q18 and Hdh-Q111 neural cell clones at E12.5 and E17.5. Primary cells from the striatal primordia were dissociated and clonally expanded for 7DIV. Hdh-Q18 (*A* and *B*) and Hdh-Q111 (*C* and *D*) clonal sections were examined at E12.5 (*A* and *C*) and at E17.5 (*B* and *D*) for apoptosis using TUNEL assay and DAPI counterstained for assessment of cell numbers. (Scale bar, 25 μm in *D*.) (*E*) Bars represent the percentage $\pm$ 95% CI of TUNEL positive cells in each experimental condition. *, *P* value corresponds to <0.05.

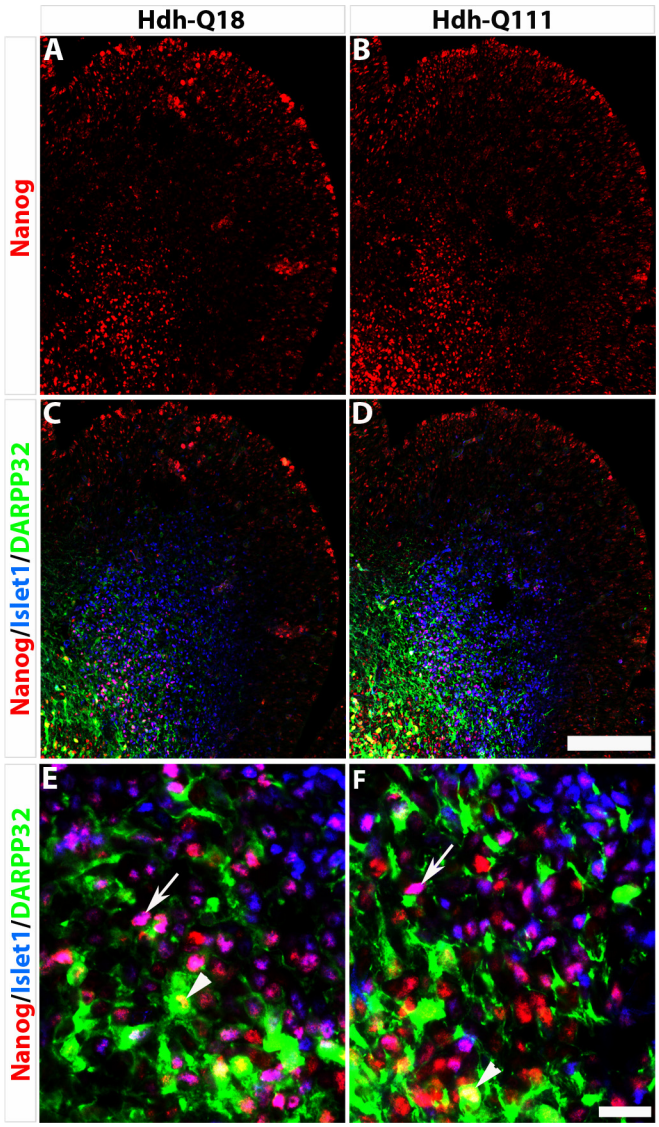

Fig. S5. The core PP factor, Nanog is extensively expressed in the Hdh-Q18 and the Hdh-Q111 striatal anlagen at E14.5 (*A* and *B*). Immunoreactivity for Nanog is observed in both the germinative and the mantle regions of the striatum. Nanog expression colocalized with the MSN markers, Islet1 and DARPP32 (*C* and *D*). *E* and *F* correspond to a higher magnification field of the mantle revealing the coexpression of Nanog with Islet1 (arrows) and DARPP32 (arrowheads). (Scale bar, 200 μm in *D* and 20 μm in *F*.)

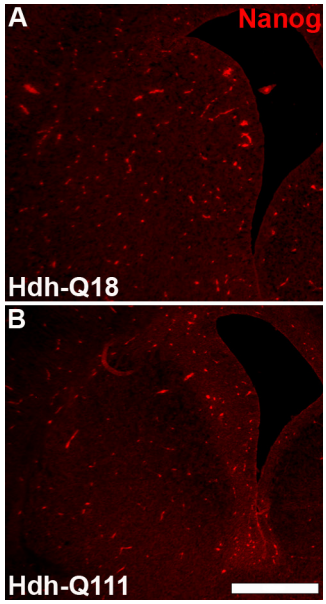

Fig. S6. Immunofluorescence microscopy does not reveal the expression of Nanog protein in neural cell species within the E17.5 striatum. Immunofluorescence micrographs of Hdh-Q18 (*A*) and Hdh-Q111 (*B*) specimens using an anti-Nanog antibody. (Scale bar, 100 μm in *B*.)

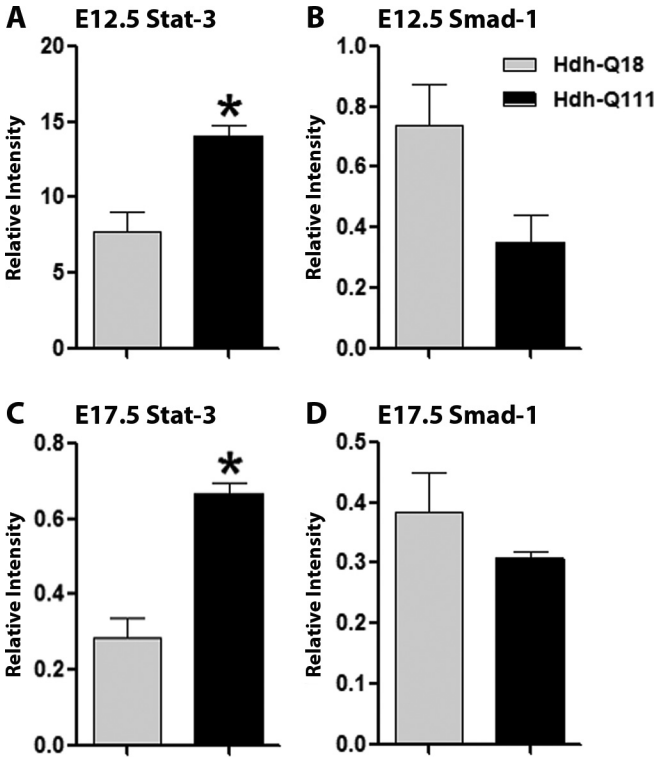

Fig. S7. The striatal anlagen of Hdh-Q111 embryos displayed increased levels of active Stat3 but not Smad1. Protein nuclear fraction from E12.5 (*A* and *B*) and E17.5 (*C* and *D*) striatal anlagen were immunoblotted with antiphospho-Stat3 (*A* and *C*) and antiphospho-Smad1 (*B* and *D*) antibodies. Each bar corresponds to the mean ± SEM. of four independent biological replicates. *, all *P* values correspond to <0.05.

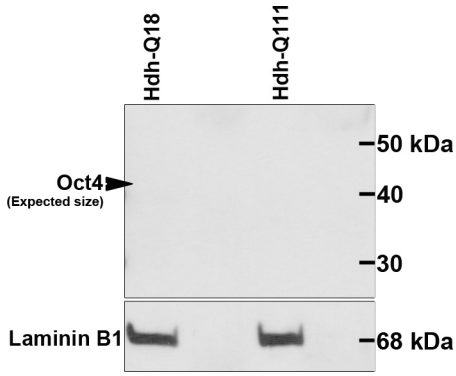

Fig. S8. Absence of Oct4 in nuclear fractions of the E12.5 striatal primordium. Protein nuclear fractions from E12.5 Hdh-Q18 and Hdh-Q111 specimens were immunoblotted using an anti-Oct4 antibody and laminin B1 as control.